Neonatal rhinovirus infection induces mucous metaplasia and airways hyperresponsiveness

Dina Schneider[1], **Jun Y. Hong**, **Antonia P. Popova**[1], **Emily R. Bowman**[1], **Marisa J. Linn**[1], **Alan M. McLean**[1], **Ying Zhao**[1], **Joanne Sonstein**[2,5], **J. Kelley Bentley**[1], **Jason B. Weinberg**[1], **Nicholas W. Lukacs**[4], **Jeffrey L. Curtis**[2,5], **Uma S. Sajjan**[1], and **Marc B. Hershenson**[1,4,*]

[1]Department of Pediatrics and Communicable Diseases, University of Michigan Medical School, Ann Arbor, MI

[2]Department of Internal Medicine, University of Michigan Medical School, Ann Arbor, MI

[3]Department of Pathology, University of Michigan Medical School, Ann Arbor, MI

[4]Department of Molecular and Integrative Physiology, University of Michigan Medical School, Ann Arbor, MI

[5]The Medical Service, VA Ann Arbor Health System, Ann Arbor, MI

Abstract

Recent studies link early rhinovirus (RV) infections to later asthma development. We hypothesized that neonatal RV infection leads to an IL-13-driven asthma-like phenotype in mice. BALB/c mice were inoculated with RV1B or sham on day 7 of life. Viral RNA persisted in the neonatal lung up to 7 days after infection. Within this time frame, IFNs-α, -β and -γ peaked 1 day after infection, whereas IFN-λ levels persisted. Next, we examined mice on day 35 of life, 28 days after initial infection. Compared to sham-treated controls, virus-inoculated mice demonstrated airways hyperresponsiveness. Lungs from RV-infected mice showed increases in several immune cell populations, as well as the percentages of CD4-positive T cells expressing IFN-γ and of NKp46/CD335+, TCR-β+ cells expressing IL-13. Periodic acid-Schiff and immunohistochemical staining revealed mucous cell metaplasia and muc5AC expression in RV1B- but not sham-inoculated lungs. Mucous metaplasia was accompanied by induction of gob-5, MUC5AC, MUC5B and IL-13 mRNA. By comparison, adult mice infected with RV1B showed no change in IL-13 expression, mucus production or airways responsiveness 28 days after infection. Intraperitoneal administration of anti-IL13 neutralizing antibody attenuated RV-induced mucous metaplasia and methacholine responses, and IL-4R null mice failed to show RV-induced mucous metaplasia. Finally, neonatal RV increased the inflammatory response to subsequent allergic sensitization and challenge. We conclude that neonatal RV1B infection leads to persistent airways inflammation, mucous metaplasia and hyperresponsiveness which are mediated, at least in part, by IL-13.

[*]Address correspondence to: Marc B. Hershenson, M.D., University of Michigan Medical School, Medical Science Research Building 2, 1150 W. Medical Center Drive, Room 3570B, Ann Arbor, MI 48109-5688, Phone: (734) 936-4200, Fax: (734) 764-3200; mhershen@umich.edu.

INTRODUCTION

Wheezing-associated acute respiratory viral infections in infancy, particularly those caused by respiratory syncytial virus (RSV) (1, 2), have been long considered risk factors for asthma. However, recent studies suggest a possible role for human rhinovirus (RV) in the pathogenesis of asthma. RV is the virus most commonly associated with acute respiratory hospitalizations in infants and young children (3). Results from the Childhood Origins of Asthma (COAST) study suggest that, in patients with a family history of asthma, wheezing-associated illness with RV is the most important risk factor for subsequent asthma development (4, 5). In another study of infants hospitalized for respiratory infection-associated wheezing, RV was associated with the development of asthma (6) in contrast to RSV which was negatively associated with later childhood asthma (7). On the other hand, while it conceivable that respiratory viral infection might lead to the development of asthma by damaging the developing airways or altering the immune response, viral infections may simply reveal a pre-existing tendency for asthma.

A number of rodent models aiming to elucidate the mechanisms linking early life viral respiratory infections to asthma have been developed. BALB/c mice infected with RSV at less than one week of age show more mucus-producing cells in the airways, mild airway tissue eosinophilia, elevated IL-13 production and airway cholinergic hyperresponsiveness (8). Mice infected with RSV at one week of age also show airways hyperresponsiveness and IL-13 production which persists 69 days after infection (9). One-to-two-day old BALB/c mice infected with pneumonia virus of mice (PVM), a natural mouse pathogen that is closely related to human RSV (10), show airway lymphocytic inflammation, modest goblet cell metaplasia and airways hyperresponsiveness at seven weeks of age that is dependent on IL-4 receptor signaling (10).

Chronic airway hyperresponsiveness and goblet cell hyperplasia following viral infection has also been shown in mature C57BL6/J mice infected with Sendai virus (murine parainfluenza virus type 1)(11). In these mice, IL-13 production by natural killer (NK) T cells and alternatively-activated macrophages is responsible for persistent mucous metaplasia (12).

Despite the association of early-life RV infections with asthma development in children (4–6), the effects of neonatal RV infection have not been tested in an animal model. We have recently developed a mouse model of RV infection employing RV1B, a minor group virus which binds to low-density lipoprotein family receptors. In this model, RV1B replicates in the lungs of mature mice and induces a robust interferon (IFN) response (13). In mice with pre-existing allergic airways disease, alternatively polarized macrophages are in part responsible for RV-induced airway inflammation and hyperresponsiveness (14). In the present study, we tested the early and late effects of RV1B infection in neonatal mice, focusing on the role of IL-13. We also examined the effects of RV infection on NK T cell IL-13 expression and macrophage polarization.

METHODS

Generation of RV

RV1B (ATCC, Manassas, VA) were grown in HeLa cells, concentrated, partially purified and titered as described (15). Similarly concentrated and purified HeLa cell lysates were used for sham infection. Fifty percent tissue culture infectivity doses ($TCID_{50}$) were determined by the Spearman-Karber method.

RV exposure

Experiments were approved by the Institutional Animal Care and Use Committee. Seven day-old BALB/c or BALB/c-*Il4ra^{tm1Sz}*/J mice (Jackson Laboratories, Bar Harbor, MA) were inoculated intranasally with 15 μl of 2×10^8 $TCID_{50}$/ml RV1B or an equal volume of sham. For selected experiments, 8 week-old BALB/c mice were inoculated with 45 μl of 2×10^8 $TCID_{50}$/ml RV1B or an equal volume of sham (13).

Lung inflammation

To quantify inflammatory cells, lung digests were minced, lysed in collagenase type IV (Gibco Invitrogen, Carlsbad, CA) and strained through 70 μm nylon mesh (BD Falcon, San Jose, CA)(16). The pellet was treated with red blood cell lysis buffer (BD Pharmingen, San Diego, CA) and leukocytes enriched by spinning the cells through 20% Percoll (Sigma-Aldrich, St. Louis, MO). Cytospins were stained with Diff-Quick (Dade Behring, Newark, DE) and differential counts determined from 200 cells.

Histology and immunohistochemistry

Lungs were fixed with 10% formaldehyde and paraffin embedded. Blocks were sectioned at 500 μm intervals at a thickness of 5 μm. Sections were stained with periodic acid-Schiff (PAS, Sigma-Aldrich) to visualize mucus accumulation. Additional sections were immunostained for goat anti-mouse muc5AC or its isotype control (Santa Cruz Biotechnology, Santa Cruz, CA), labeled with biotinylated anti-goat IgG (Vector Labs, Burlingame, CA) and developed using the Vectastain Elite ABC kit (Vector Labs) and diaminobenzidine (Sigma-Aldrich) as a substrate. The number of PAS-positive cells per basement membrane length and alveolar chord length were determined using NIH ImageJ analysis software (Bethesda, MD), as described (17).

Quantitative real time PCR

Whole lung RNA was extracted with RNeasy (Qiagen, Valencia, CA) and analyzed by quantitative real time PCR using specific primers and probes. Signals were normalized to GAPDH.

Measurement of lung cytokines

IL-4, IL-5 and IL-13 protein levels were measured by immune bioplex assay (BioRad, Hercules, CA).

Flow cytometry

Staining and analysis by flow cytometry were performed as described (18). Cells were analyzed on an LSR II flow cytometer (BD Biosciences, San Jose, CA) equipped with 488-nm blue, 405-nm violet, and 633-nm red lasers. Data were collected on an HP XW4300 Workstation (Hewlett-Packard, Palo Alto, CA) using FACSDiva software (BD Biosciences) with automatic compensation and were analyzed using FlowJo software (Tree Star, Ashland, OR). A range of cells (10,000–100,000) were analyzed per sample. Isotype-matched irrelevant control monoclonal antibodies were tested simultaneously in all experiments. We used monoclonal antibodies against the following antigens (clones and fluorochromes shown in brackets): Ly6G {1A8; fluorescein isothiocyanate (FITC) or phycoerythrin (PE)}, Siglec-F {E50-2440; PE} and CD19 {1D3; Allophycocyanin-Cyanine 7 (APC-Cy7)} (each from BD Pharmingen, San Jose, CA); CD4 {GK1.5 PE-Cy7}, CD11b {M1/70 Alexa Fluor 700 (AF700)}, CD11c {N418 Pacific Blue}, IFN-γ {XMG1.2 Pacific Blue}, IL-13 {eBio13A AF647}, NKp46/CD335 {29A1.4 eFluor 660} and TCR-β {H57-597 FITC or PE} (each from eBioscience, San Diego, CA); CD206 (MR5D3 AF647)(AbD Serotec, Raleigh, NC). Appropriate isotype-matched controls were used in all experiments

For intracellular staining, freshly isolated aliquots of the lung mince were stimulated for 5 hours at 37° C in 5% CO_2 with PMA (50 ng/ml) and ionomycin (1 ug/ml) in the presence of brefeldin A. The lung minces were washed and the cell pellets resuspended in Dulbecco's PBS. To eliminate potential artifacts due to dead cell contamination, the cells were first stained with Aqua Live/Dead Fixable Dead Cell Stain Kit (Invitrogen Corperation, Carlsbad, CA) and then stained for surface antibodies as above. The lung mince cells were fixed, permeabilized and then incubated with anti-mouse IFN-γ, IL-13 and CD206 according to the eBioscience protocol for intracellular immunofluorescent staining of cells for flow cytometry.

Airways responsiveness

Airway cholinergic responsiveness was assessed by measuring changes in total respiratory system resistance in response to increasing doses of nebulized methacholine. Mice were anesthetized with pentobarbital. Resistance was measured plethysmographically (Buxco, Wilmington, NC).

IL-13 neutralization

For IL-13 neutralization, 30 μg of goat anti- mouse IL-13 or normal goat IgG (R&D Systems, Minneapolis, MN) were administered intraperitoneally on days 0, 2, 4 and 6 post-infection. Mice were sacrificed for analysis 28 days after initial RV infection.

Ovalbumin (OVA) sensitization and challenge

For OVA sensitization, mice were injected intraperitoneally on days of life 17 and 24 with 100 μl PBS or a solution of alum and 50μg endotoxin-free OVA (Sigma-Aldrich). Next, mice were challenged intranasally with 25 μl of PBS or 50 μg OVA in PBS on days of life 32, 33 and 34. Mice were studied one day after the final challenge.

Data analysis

Data are represented as mean±SEM. Statistical significance was determined by unpaired *t* test, rank sum test, or two-way analysis of variance (ANOVA) as appropriate. Differences were pinpointed by Newman-Keuls' multiple range test.

RESULTS

RV1B infection elicits IFN responses and inflammation in neonatal mice

We initially characterized the response to viral inoculation in 7 day-old BALB/c pups. Pups were intranasally infected with RV1B or sham control, and lungs were harvested for analysis 1–7 days after infection. Positive-strand viral RNA persisted in the mouse lung up to 7 days after infection (Figure 1A). The sustained level of viral copies three days after infection strongly suggests that RV causes a replicative infection in neonatal mice. Virus was not detected greater than 7 days following infection.

mRNAs encoding IFNs-α, -β and γ were each strongly induced at 1 d after RV1B infection, but not after sham inoculation (Figure 1B). IFN-α, -β and-γ levels decreased thereafter. In contrast, IFN-λ mRNA levels remained elevated through day 7. IFN-λ receptors are largely restricted to cells of epithelial origin (19) and IFN-λ receptor knockout mice show attenuated antiviral responses to double-stranded RNA (20). It is therefore conceivable that double-stranded RNA, released from RV-infected epithelial cells, stimulates further IFN-λ production.

Lung differential cell counts revealed modest but statistically significant increases in the numbers of neutrophils on days 3, 5 and 7, and in the number of macrophages on days 5 and 7 post-infection (Figure 2A–D). In addition, lymphocytes and eosinophils were increased 7 days after infection. Nevertheless, histology showed minimal cellular infiltration of the lungs after RV infection in neonatal animals (Figure 2E, 2F).

Lungs were examined for selected mRNAs encoding pro-inflammatory cytokines and chemokines. Based on the early neutrophilic response to RV infection, we chose to examine three neutrophil chemoattractants (CXCL1, CXCL2 and TNF-α), each of which are induced by RV1B infection in mature mice (21). mRNAs encoding CXCL1, CXCL2 and TNF-α were each increased compared to sham-inoculated mice (Figure 3). mRNA expression of IL-13, which has previously been shown to be induced by neonatal RSV infection (8), was also increased.

Neonatal RV1B infection induces airway hyperresponsiveness, inflammation and mucus accumulation

We examined the airway cholinergic responsiveness of sham- and RV-exposed mice on day 35 of life (28 days after infection). We detected no viral RNA in either treatment group at 28 days after infection (not shown). There was no difference in weight between sham and RV-infected mice at this time point (sham, 29.5 ± 1.9 g; RV, 29.4 ± 2.9 g). However, there was a significant increase in methacholine responsiveness in mice infected with RV as neonates (Figure 4A). In contrast, mature mice infected with RV1B showed no increase in airways responsiveness 28 days after infection.

To understand the change in responsiveness, we examined the lungs of 35 day-old mice infected as neonates. Most airways were histologically normal. Again, differences in inflammatory cells between sham- and RV-infected mice were slight. Selected airways from RV-infected mice showed a modest amount of peribronchial inflammation (Figures 4B, 4C). In addition, RV-infected mice showed rare localized collections of lymphocytes in the peribronchial, perivascular and subpleural spaces (Figures 4D, 4E). Compared to sham-infected mice, lung digests of RV-infected mice showed a small but significant increase in the percentage of neutrophils (sham, $3.3 \pm 1.1\%$ of total; RV, $12.5 \pm 1.9\%$, mean$\pm$SEM, $p < 0.001$, unpaired t test). Lungs of mice undergoing neonatal RV infection also demonstrated modest increases in total neutrophils, macrophages, lymphocytes and eosinophils (Figure 4F). There was no difference in mean alveolar chord length between sham- and RV-infected mice (sham, 25.3 ± 0.2 μ; RV, 24.9 ± 0.9 μ, $p = 0.71$). The minimal cellular infiltration of the lungs after RV infection in neonatal animals, particularly at later time points when airways responsiveness is increased, suggests that other mechanisms are responsible for the observed airways hyperresponsiveness.

To learn more about changes in leukocyte subsets following RV infection, we conducted flow cytometry of cells from minced lungs obtained from mice 3 weeks after neonatal infection, focusing on NK T cells and macrophage polarization. We found increases in Gr1-neutrophils and Gr1-, SigF-double-positive eosinophils, CD4-positive T cells, CD19-positive B cells and CD11b-positive cells within monocyte/macrophage gates compared to sham controls (Figure 5A–F). CD11b-positive cells from RV-infected mice showed a significant increase in CD206 expression (Figure 5G), indicating alternative macrophage polarization. When cells were co-stained with antibodies against IFN-γ and IL-13, lung cells from RV-infected mice showed increases in the percentage of CD4-positive T cells expressing IFN-γ (Figure 5H), and the percentage of NKp46/CD335-positive TCR-β-positive cells (NK T cells) expressing IL-13 (Figure 5I). Finally, CD11b-positive cells did not express IL-13 (data not shown).

We then examined PAS staining. Lungs from 35-day old mice inoculated with sham on day 7 of life showed a range of PAS staining ranging from no signal to patches of dense staining in the large airways (Figures 6A, 6B). In contrast, mice infected with RV at day 7 of life and studied at day 35 showed some large airways which were completely filled with PAS-positive epithelial cells, as well as PAS-staining in the medium-sized and small airways (Figures 6C, 6D). Sham- and RV-infected mature mice showed only rare PAS-positive cells 28 days after treatment (not shown). Mucus-secreting cells in the large airways were assessed 14, 21 and 28 days after neonatal infection by counting PAS-positive cells per basement membrane length. RV-infected mice showed significantly increased PAS staining (Figure 6E). We also examined PAS staining 60 and 100 days after neonatal sham or RV treatment, on days 67 and 107 of life. At these time points, both groups showed only sparse PAS staining in the large airways, indicating that RV-induced mucous metaplasia had mostly resolved. However, some small airways of RV-infected 67 day-old mice continued to show PAS staining (Figure 6F). Immunohistochemical staining for muc5AC confirmed increased mucus expression in the large and small airways of RV-treated mice (Figures 6F–I).

We examined the time course of the mucus-related genes *gob5*, *muc5AC* and *muc5B*. Given the sufficiency of pulmonary IL-13 expression for mucus hypersecretion in transgenic mice (22), we also examined the time course of this Th2 cytokine. The mRNA levels of genes related to mucus production were increased in mice infected as neonates, but not mice infected as adults (Figures 7A–C). A similar pattern was observed for IL-13 mRNA, with significant increases on days 7, 14 and 21 (but not 28) after infection (Figure 7D). Lung levels of the Th2 cytokines IL-4, IL-5 and IL-13 were each significantly increased three weeks after RV inoculation (Figure 7E).

IL-13 neutralization attenuates RV-induced mucus accumulation and airways responsiveness

We hypothesized that IL-13 is required for mucus hypersecretion and airways hyperresponsiveness. We therefore administered neutralizing antibody to IL-13 or non-immune serum days 0–6 post-RV infection. As noted previously, airways responsiveness was increased in BALB/c mice 28 days after neonatal RV infection. However, mice treated with anti-IL-13 showed a decreased level of methacholine responsiveness (Figure 8A). Anti-IL-13 decreased the number of PAS-positive cells in the small airways, as defined by a circumference < 3 mm (Figure 8B). Administration of anti-IL-13 had no effect on lung digest differential cell counts (not shown).

IL-4 receptor null mice show reduced mucous metaplasia in response to neonatal RV infection

BALB/c-*Il4ratm1Sz*/J mice (23) were inoculated with sham or RV1B, as described above. In contrast to wild-type mice, RV1B-treated IL-4 receptor null mice showed no increase in PAS staining compared to sham-treated mice (Figure 9A–C; compare to Figures 6C and 6D). In addition, there was no significant increase in gob5, muc5AC, muc5B or IL-13 mRNA expression (Figure 9D; compare to Figure 7).

Effect of early RV infection on the response to OVA sensitization and challenge

Mice were inoculated with sham or RV on day 7 of life, sensitized to PBS or OVA on days 17 and 24, and challenged with PBS or OVA on days 32 and 34. Mice were studied one day after the final challenge. Neonatal RV infection increased OVA-induced airway inflammation (Figures 10A, 10B). Prior RV infection increased lung digest neutrophil and macrophage, but not lymphocyte or eosinophil counts (Figures 10C). Finally, prior neonatal

RV infection increased airways responsiveness following allergen sensitization and challenge (Figure 10D).

DISCUSSION

We demonstrate that, unlike mature mice, BALB/c mice inoculated with RV1B at seven days of age display airways hyperresponsiveness, mucus metaplasia and IL-13 production which lasts at least one month after infection. These data suggest that early life infection with RV can induce a prolonged state of airway pathology which recapitulates three hallmark features of allergic asthma.

It has previously been shown that infection of BALB/c mice shortly after birth with RSV and the closely-related PVM causes persistent modest goblet cell metaplasia, airways hyperresponsiveness and IL-13 production (9, 24). Infection of mature mice with RSV and PVM each result in the loss of cilia and sloughing of epithelial cells into the airway, airway wall edema, and packing of the airway lumen with polymorphonuclear leukocytes, fibrin, lymphocytes and mucus (10, 25), Similar findings are present in infants dying of RSV bronchiolitis (26). On this basis, perhaps it is not surprising that RSV infection causes long-lasting effects on airway function. On the other hand, RSV infection of one-to-two day-old mice induced relatively modest airway changes (24), perhaps because of an attenuated immune response, which is required for full-blown RSV-induced clinical illness (27).

In contrast to RSV, RV typically infects small clusters of cells in the airway epithelium (28) and elicits minimal, if any, cytotoxicity (29). In mature mice, RV infection causes modest neutrophilic and lymphocytic inflammation (13) and, as shown in this report, no mucous metaplasia. In the present study, lung digests from BALB/c mice infected on day 7 of life showed modest infiltration of the airways with neutrophils, lymphocytes, macrophages and eosinophils. Similarly, at age 35 days, the lungs of mice undergoing neonatal RV infection showed only a minor amount of peribronchial inflammation, with small but significant increases in total neutrophils, macrophages and lymphocytes. Thus, the amount of cellular infiltration of the airways is unlikely to be the sole cause of the observed airways hyperresponsiveness.

We also observed peribronchial, perivascular and subpleural collections of lymphocytes in the lungs of RV- but not sham-infected mice. These collections, which resemble bronchus-associated lymphoid tissue (BALT), are only occasionally present in normal mice, but may be induced by sensitization and challenge with heat-killed *Pseudomonas aeruginosa* (30) or by heterologous viral infections (31, 32). BALT is also spontaneously increased in the peribronchial and perivascular lung tissue of mice deficient for the chemokine receptor CCR7 (33, 34). In humans, BALT is commonly present in infants but not in normal adult lungs (35). The presence of BALT-like infiltrates is evidence of an adaptive immune response against RV infection.

RV infection of immature mice also induced significant mucous metaplasia that was present 14 days after infection and persisted until 28 days after infection. Consistent with this, RV-infected immature mice showed significant increases in mRNAs encoding the gel-forming glycoproteins MUC5AC and MUC5B. MUC5AC protein was also increased. Gob-5 (mCLCA3), a member of the calcium-activated chloride channel family which drives mucin release (36, 37) was also significantly increased. Neither sham-treated immature mice nor mature mice showed such increases. Like RV, RSV infection increases the number of mucus-producing cells in immature but not mature mice (8). Together, these data suggest that the newborn airway is more susceptible to virus-induced mucous metaplasia.

Gob-5 expression and mucus secretion are positively regulated by the Th2 cytokines IL-13, IL-10 and IL-9 (22, 38, 39), and IL-10-induced mucous metaplasia is IL-13-dependent (38). Persistent mucous metaplasia and airways hyperresponsiveness does not occur in PVM-infected IL-4 receptor knockout mice, implying a requirement for IL-13 in this process. We therefore examined the mRNA expression of IL-13 in RV-infected mice. Quantitative PCR demonstrated a biphasic increase in IL-13 mRNA expression (Figure 3D), with an initial induction immediately after RV infection and a second peak 21 days after infection (Figure 7D). Administration of anti-IL-13 neutralizing antibody significantly decreased PAS staining in the small airways and partially decreased airways responsiveness. Finally, IL-4R null mice failed to show RV-induced mucous metaplasia, implicating IL-13 in the pathogenesis of persistent airway changes in RV-infected neonatal mice.

Chronic airway hyperresponsiveness and goblet cell hyperplasia following viral infection was first shown in C57BL6/J strain infected with Sendai virus (murine parainfluenza virus type 1)(11), a negative sense, single-stranded RNA virus. In these mice, IL-13 production by natural killer (NK) T cells and alternatively-activated macrophages is responsible for persistent mucous metaplasia (12). We have recently shown that alternatively polarized macrophages are responsible for RV-induced airway inflammation and hyperresponsiveness in mature mice with allergic airways disease (14). In the present study, we found increased expression of CD206, also known as macrophage mannose receptor 1 and C-type lectin domain family 13 member D (CLEC13D), in CD11b-positive macrophages, indicative of a switch in macrophage activation state. Alternative macrophage activation has been demonstrated to be IL-13-dependent in *Cryptococcus neoformans*-infected mice (40). We also found an increase in the percentage of CD335-positive, T cell receptor-β-positive cells expressing IL-13. Together, these results are consistent with the notion that IL-13, produced by NK T cells, plays a significant role in chronic mucus metaplasia and hyperresponsiveness following viral infection. Other mechanisms are possible, however. We have not excluded the possibility that IL-13-producing CD4-positive Th2 lymphocytes play a role. It is therefore conceivable that RV infection has direct effects on airway epithelial cell mucus production. RV infection of NCI-H292 airway epithelial cells induces TLR3- and epidermal growth factor receptor-dependent MUC5AC expression (41). We have also noticed that RV infection of primary airway epithelial cells grown at air-liquid interface induces mucus metaplasia (U. Sajjan, M. Hershenson, unpublished data). In addition, the pro-inflammatory cytokine IL-17A has been shown to regulate airway epithelial cell MUC5AC and MUC5B expression via an IL-6 paracrine loop (42). Finally, while it is conceivable that early RV infection increases airway responsiveness by inducing subtle alterations in airway and parenchymal development (43), Importantly, neonatal RV infection had no effect on lung alveolarization.

As noted above, infection of mature mice failed to induce mucous metaplasia or long-lasting airways hyperresponsiveness as it did in neonatal mice. The mechanisms underlying this age-dependent effect are unclear. First, it is conceivable that neonatal mice are more susceptible to viral infection, leading to exaggerated airway effects. It has previously been shown that the activation and entry of neonatal T cells into the lungs is delayed after influenza infection (44). In the present study, RV copy number was sustained for three days in neonatal mice, and lung lymphocyte infiltration did not increase until 7 days after infection. This contrasts with mature mice in which viral copy number peaks 24 h after infection and lymphocyte infiltration increases one day after infection. In addition, neutrophilic inflammation and IFN-γ expression by $CD4^+$ T cells persisted for weeks after neonatal infection. Together, these results suggest a delayed and prolonged response to acute viral infection in neonatal animals. Second, the neonatal airway epithelium may be more susceptible to rhinovirus infection than the mature epithelium. Mucous metaplasia has been shown to increase susceptibility of the airway epithelium to RV infection (45). In rhesus

monkeys, goblet cells in the trachea decrease in abundance with increasing age (46). We noted that sham-infected 35 day-old mice show a range of PAS staining, extending from no signal to patches of dense staining in the large airways, whereas sham-infected 8 week-old mice show only rare PAS-positive cells. Third, it is possible that early life viral infection causes mucous metaplasia and airways hyperresponsiveness by augmenting or maintaining the neonatal immature response, which is skewed towards a Th2 phenotype (47–49). The relatively high IL-13 levels in both sham- and RV-treated immature mice are consistent with Th2 polarization.

Neonatal RV infection also enhanced the inflammatory response to allergen sensitization and challenge. Prior infection with RSV has been shown to increase subsequent allergic airways responses in both immature (9) and mature mice (50). Interestingly, in contrast to the previous study of neonatal RSV infection, prior infection with RV significantly increased OVA-induced neutrophilic inflammation. The mechanisms by which allergen exposure induces neutrophilic airways inflammation have not been well-studied, but may involve the activation of the IL-17/IL-23 axis (51, 52).

Finally, we would like to note that the effects of neonatal RV infection appeared to fade with time, with mucous metaplasia substantially reduced by 60 days after infection and absent by 100 days after infection. Since babies are exposed to RV numerous times during infancy, it is conceivable that there could be additive or synergistic effects of infection over time.

We conclude that RV1B infection of neonatal BALB/c mice leads to airways inflammation, mucous metaplasia and hyperresponsiveness which are mediated at least in part, by IL-13. These results are consistent with the notion that, under certain circumstances, early infection with RV may play a causal role in the development of asthma.

Acknowledgments

References

1. Sigurs N, Bjarnason R, Sigurbergsson F, Kjellman B. Respiratory syncytial virus bronchiolitis in infancy is an important risk factor for asthma and allergy at age 7. Am J Respir Crit Care Med. 2000; 161:1501–1507. [PubMed: 10806145]

2. Sigurs N, Gustafsson PM, Bjarnason R, Lundberg F, Schmidt S, Sigurbergsson F, Kjellman B. Severe respiratory syncytial virus bronchiolitis in infancy and asthma and allergy at age 13. Am J Respir Crit Care Med. 2005; 171:137–141. [PubMed: 15516534]

3. Miller EK, Lu X, Erdman DD, Poehling KA, Zhu Y, Griffin MR, Hartert TV, Anderson LJ, Weinberg GA, Hall CB, Iwane MK, Edwards KM. Rhinovirus-associated hospitalizations in young children. J Infect Dis. 2007; 195:773–781. [PubMed: 17299706]

4. Lemanske RF, Jackson DJ, Gangnon RE, Evans MD, Li Z, Shult PA, Kirk CJ, Reisdorf E, Roberg KA, Anderson EL, Carlson-Dakes KT, Adler KJ, Gilbertson-White S, Pappas TE, Dasilva DF, Tisler CJ, Gern JE. Rhinovirus illnesses during infancy predict subsequent childhood wheezing. J Allergy Clin Immunol. 2005; 116:571–577. [PubMed: 16159626]

5. Jackson DJ, Gangnon RE, Evans MD, Roberg KA, Anderson EL, Pappas TE, Printz MC, Lee WM, Shult PA, Reisdorf E, Carlson-Dakes KT, Salazar LP, DaSilva DF, Tisler CJ, Gern JE, Lemanske RF Jr. Wheezing rhinovirus illnesses in early life predict asthma development in high-risk children. Am J Respir Crit Care Med. 2008; 178:667–672. [PubMed: 18565953]

6. Kotaniemi-Syrjänen A, Vainionpää R, Reijonen TM, Waris M, Korhonen K, Korppi M. Rhinovirus-induced wheezing in infancy--the first sign of childhood asthma? J Allergy Clin Immunol. 2003; 111:66–71. [PubMed: 12532098]

7. Reijonen TM, Kotaniemi-Syrjanen A, Korhonen K, Korppi M. Predictors of asthma three years after hospital admission for wheezing in infancy. Pediatrics. 2000; 106:1406–1412. [PubMed: 11099596]

8. Dakhama A, Park JW, Taube C, Joetham A, Balhorn A, Miyahara N, Takeda K, Gelfand EW. The enhancement or prevention of airway hyperresponsiveness during reinfection with respiratory syncytial virus is critically dependent on the age at first infection and IL-13 production. J Immunol. 2005; 175:1876–1883. [PubMed: 16034131]

9. You D, Becnel D, Wang K, Ripple M, Daly M, Cormier S. Exposure of neonates to respiratory syncytial virus is critical in determining subsequent airway response in adults. Respir Res. 2006; 7:107. [PubMed: 16893457]

10. Rosenberg HF, Domachowske JB. Pneumonia virus of mice: severe respiratory infection in a natural host. Immunol Lett. 2008; 118:6–12. [PubMed: 18471897]

11. Walter MJ, Morton JD, Kajiwara N, Agapov E, Holtzman MJ. Viral induction of a chronic asthma phenotype and genetic segregation from the acute response. J Clin Invest. 2002; 110:165–175. [PubMed: 12122108]

12. Kim EY, Battaile JT, Patel AC, You Y, Agapov E, Grayson MH, Benoit LA, Byers DE, Alevy Y, Tucker J, Swanson S, Tidwell R, Tyner JW, Morton JD, Castro M, Polineni D, Patterson GA, Schwendener RA, Allard JD, Peltz G, Holtzman MJ. Persistent activation of an innate immune response translates respiratory viral infection into chronic lung disease. Nat Med. 2008; 14:633–640. [PubMed: 18488036]

13. Newcomb DC, Sajjan US, Nagarkar DR, Wang Q, Nanua S, Zhou Y, McHenry CL, Hennrick KT, Tsai WC, Bentley JK, Lukacs NW, Johnston SL, Hershenson MB. Human rhinovirus 1B exposure induces phosphatidylinositol 3-kinase-dependent airway inflammation in mice. Am J Respir Crit Care Med. 2008; 177:1111–1121. [PubMed: 18276942]

14. Nagarkar DR, Bowman ER, Schneider D, Wang Q, Shim J, Zhao Y, Linn MJ, McHenry CL, Gosangi B, Bentley JK, Tsai WC, Sajjan US, Lukacs NW, Hershenson MB. Rhinovirus infection of allergen-sensitized and -challenged mice induces eotaxin release rom functionally polarized macrophages. J Immunol. 2010; 185:2525–2535. [PubMed: 20644177]

15. Newcomb DC, Sajjan U, Nanua S, Jia Y, Goldsmith AM, Bentley JK, Hershenson MB. Phosphatidylinositol 3-kinase is required for rhinovirus-induced airway epithelial cell interleukin-8 expression. J Biol Chem. 2005; 280:36952–36961. [PubMed: 16120607]

16. Ojielo CI, Cooke K, Mancuso P, Standiford TJ, Olkiewicz KM, Clouthier S, Corrion L, Ballinger MN, Toews GB, Paine R III, Moore BB. Defective phagocytosis and clearance of pseudomonas aeruginosa in the lung following bone marrow transplantation. J Immunol. 2003; 171:4416–4424. [PubMed: 14530368]

17. Sajjan U, Ganesan S, Comstock AT, Shim J, Wang Q, Nagarkar DR, Zhao Y, Goldsmith AM, Sonstein J, Linn MJ, Curtis JL, Hershenson MB. Elastase- and LPS-exposed mice display altered responses to rhinovirus infection. Am J Physiol Lung Cell Mol Physiol. 2009; 297:L931–944. [PubMed: 19748999]

18. Osterholzer JJ, Chen GH, Olszewski MA, Curtis JL, Huffnagle GB, Toews GB. Accumulation of CD11b+ lung dendritic cells in response to fungal infection results from the CCR2-mediated recruitment and differentiation of Ly-6Chigh monocytes. J Immunol. 2009; 183:8044–8053. [PubMed: 19933856]

19. Sommereyns C, Paul S, Staeheli P, Michiels T. IFN-Lambda (IFN-λ) is expressed in a tissue-dependent fashion and primarily acts on epithelial cells in Vivo. PLoS Pathog. 2008; 4:e1000017. [PubMed: 18369468]

20. Ank N, Iversen MB, Bartholdy C, Staeheli P, Hartmann R, Jensen UB, Dagnaes-Hansen F, Thomsen AR, Chen Z, Haugen H, Klucher K, Paludan SR. An important role for type III Interferon (IFN-λ/IL-28) in TLR-induced antiviral activity. J Immunol. 2008; 180:2474–2485. [PubMed: 18250457]

21. Nagarkar DR, Wang Q, Shim J, Zhao Y, Tsai WC, Lukacs NW, Sajjan U, Hershenson MB. CXCR2 is required for neutrophilic airway inflammation and hyperresponsiveness in a mouse model of human rhinovirus infection. J Immunol. 2009; 183:6698–6707. [PubMed: 19864593]

22. Zhu Z, Homer RJ, Wang Z, Chen Q, Geba GP, Wang J, Zhang Y, Elias JA. Pulmonary expression of interleukin-13 causes inflammation, mucus hypersecretion, subepithelial fibrosis, physiologic abnormalities, and eotaxin production. J Clin Invest. 1999; 103:779–788. [PubMed: 10079098]

23. Noben-Trauth N, Shultz LD, Brombacher F, Urban JF, Gu H, Paul WE. An interleukin 4 (IL-4)-independent pathway for CD4+ T cell IL-4 production is revealed in IL-4 receptor-deficient mice. Proc Natl Acad Sci USA. 1997; 94:10838–10843. [PubMed: 9380721]

24. Siegle J, Hansbro N, Herbert C, Rosenberg H, Domachowske J, Asquith K, Foster P, Kumar R. Early-life viral infection and allergen exposure interact to induce an asthmatic phenotype in mice. Respir Res. 2010; 11:14. [PubMed: 20122285]

25. Tekkanat KK, Maassab HF, Cho DS, Lai JJ, John A, Berlin A, Kaplan MH, Lukacs NW. IL-13-induced airway hyperreactivity during respiratory syncytial virus infection is STAT6 dependent. J Immunol. 2001; 166:3542–3548. [PubMed: 11207314]

26. Johnson JE, Gonzales RA, Olson SJ, Wright PF, Graham BS. The histopathology of fatal untreated human respiratory syncytial virus infection. Mod Pathol. 2006; 20:108–119. [PubMed: 17143259]

27. Graham BS, Bunton LA, Wright PF, Karzon DT. Role of T lymphocyte subsets in the pathogenesis of primary infection and rechallenge with respiratory syncytial virus in mice. J Clin Invest. 1991; 88:1026–1033. [PubMed: 1909350]

28. Mosser AG, Vrtis R, Burchell L, Lee WM, Dick CR, Weisshaar E, Bock D, Swenson CA, Cornwell RD, Meyer KC, Jarjour NN, Busse WW, Gern JE. Quantitative and qualitative analysis of rhinovirus infection in bronchial tissues. Am J Respir Crit Care Med. 2005; 171:645–651. [PubMed: 15591468]

29. Fraenkel DJ, Bardin PG, Sanderson G, Lampe F, Johnston SL, Holgate ST. Lower airways inflammation during rhinovirus colds in normal and in asthmatic subjects. Am J Respir Crit Care Med. 1995; 151:879–886. [PubMed: 7881686]

30. Toyoshima M, Chida K, Sato A. Antigen uptake and subsequent cell kinetics in bronchus-associated lymphoid tissue. Respirology. 2000; 5:141–145. [PubMed: 10894103]

31. Chen HD, Fraire AE, Joris I, Welsh RM, Selin LK. Specific history of heterologous virus infections determines anti-viral immunity and immunopathology in the lung. Am J Pathol. 2003; 163:1341–1355. [PubMed: 14507643]

32. Nguyen YN, McGuffie BA, Anderson VE, Weinberg JB. Gammaherpesvirus modulation of mouse adenovirus type 1 pathogenesis. Virology. 2008; 380:182–190. [PubMed: 18768196]

33. Kocks JR, Davalos-Misslitz ACM, Hintzen G, Ohl L, Förster R. Regulatory T cells interfere with the development of bronchus-associated lymphoid tissue. J Exp Med. 2007; 204:723–734. [PubMed: 17371929]

34. Kallal LE, Hartigan AJ, Hogaboam CM, Schaller MA, Lukacs NW. Inefficient lymph node sensitization during respiratory viral infection promotes il-17-mediated lung pathology. J Immunol. 2010; 185:4137–4147. [PubMed: 20805422]

35. Tschernig T, Pabst R. Bronchus-associated lymphoid tissue (BALT) is not present in the normal adult lung but in different diseases. Pathobiology. 2000; 68:1–8. [PubMed: 10859525]

36. Nakanishi A, Morita S, Iwashita H, Sagiya Y, Ashida Y, Shirafuji H, Fujisawa Y, Nishimura O, Fujino M. Role of gob-5 in mucus overproduction and airway hyperresponsiveness in asthma. Proc Natl Acad Sci USA. 2001; 98:5175–5180. [PubMed: 11296262]

37. Long AJ, Sypek JP, Askew R, Fish SC, Mason LE, Williams CMM, Goldman SJ. Gob-5 contributes to goblet cell hyperplasia and modulates pulmonary tissue inflammation. Am J Respir Cell Mol Biol. 2006; 35:357–365. [PubMed: 16645179]

38. Lee CG, Homer RJ, Cohn L, Link H, Jung S, Craft JE, Graham BS, Johnson TR, Elias JA. Transgenic overexpression of interleukin (IL)-10 in the lung causes mucus metaplasia, tissue inflammation, and airway remodeling via IL-13-dependent and -independent pathways. J Biol Chem. 2002; 277:35466–35474. [PubMed: 12107190]

39. Zhou Y, Dong Q, Louahed J, Dragwa C, Savio D, Huang M, Weiss C, Tomer Y, McLane MP, Nicolaides NC, Levitt RC. Characterization of a calcium-activated chloride channel as a shared target of Th2 cytokine pathways and its potential involvement in asthma. Am J Respir Cell Mol Biol. 2001; 25:486–491. [PubMed: 11694454]

40. Muller U, Stenzel W, Kohler G, Werner C, Polte T, Hansen G, Schutze N, Straubinger RK, Blessing M, McKenzie ANJ, Brombacher F, Alber G. IL-13 induces disease-promoting type 2 cytokines, alternatively activated macrophages and allergic inflammation during pulmonary

infection of mice with Cryptococcus neoformans. J Immunol. 2007; 179:5367–5377. [PubMed: 17911623]

41. Zhu L, Lee P-k, Lee W-m, Zhao Y, Yu D, Chen Y. Rhinovirus-Induced Major airway mucin production involves a novel TLR3-EGFR-dependent pathway. Am J Respir Cell Mol Biol. 2009; 40:610–619. [PubMed: 18978302]

42. Chen Y, Thai P, Zhao YH, Ho YS, DeSouza MM, Wu R. Stimulation of airway mucin gene expression by interleukin (IL)-17 through IL-6 paracrine/autocrine loop. J Biol Chem. 2003; 278:17036–17043. [PubMed: 12624114]

43. Castleman WL. Alterations in pulmonary ultrastructure and morphometric parameters induced by parainfluenza (Sendai) virus in rats during postnatal growth. Am J Pathol. 1984; 114:322–335. [PubMed: 6320651]

44. Lines JL, Hoskins S, Hollifield M, Cauley LS, Garvy BA. The migration of T Cells in response to influenza virus is altered in neonatal mice. J Immunol. 185:2980–2988. [PubMed: 20656925]

45. Lachowicz-Scroggins ME, Boushey HA, Finkbeiner WE, Widdicombe JH. Interleukin-13-induced mucous metaplasia increases susceptibility of human airway epithelium to rhinovirus infection. Am J Respir Cell Mol Biol. 2010; 43:652–661. [PubMed: 20081054]

46. Van Winkle LS, Fanucchi MV, Miller LA, Baker GL, Gershwin LJ, Schelegle ES, Hyde DM, Evans MJ, Plopper CG. Epithelial cell distribution and abundance in rhesus monkey airways during postnatal lung growth and development. J Appl Physiol. 2004; 97:2355–2363. [PubMed: 15298983]

47. Li L, Lee HH, Bell JJ, Gregg RK, Ellis JS, Gessner A, Zaghouani H. IL-4 utilizes an alternative receptor to drive apoptosis of Th1 cells and skews neonatal immunity toward Th2. Immunity. 2004; 20:429–440. [PubMed: 15084272]

48. Goriely S, Vincart B, Stordeur P, Vekemans J, Willems F, Goldman M, De Wit D. Deficient IL-12(p35) gene expression by dendritic cells derived from neonatal monocytes. J Immunol. 2001; 166:2141–2146. [PubMed: 11160266]

49. Lee HH, Hoeman CM, Hardaway JC, Guloglu FB, Ellis JS, Jain R, Divekar R, Tartar DM, Haymaker CL, Zaghouani H. Delayed maturation of an IL-12–producing dendritic cell subset explains the early Th2 bias in neonatal immunity. J Exp Med. 2008; 205:2269–2280. [PubMed: 18762566]

50. Schwarze J, Hamelmann E, Bradley KL, Takeda K, Gelfand EW. Respiratory syncytial virus infection results in airway hyperresponsiveness and enhanced airway sensitization to allergen. J Clin Invest. 1997; 100:226–233. [PubMed: 9202075]

51. Hellings PW, Kasran A, Liu Z, Vandekerckhove P, Wuyts A, Overbergh L, Mathieu C, Ceuppens JL. Interleukin-17 orchestrates the granulocyte influx into airways after allergen inhalation in a mouse model of allergic asthma. Am J Respir Cell Mol Biol. 2003; 28:42–50. [PubMed: 12495931]

52. Wilson RH, Whitehead GS, Nakano H, Free ME, Kolls JK, Cook DN. Allergic sensitization through the airway primes Th17-dependent neutrophilia and airway hyperresponsiveness. Am J Respir Crit Care Med. 2009; 180:720–730. [PubMed: 19661246]
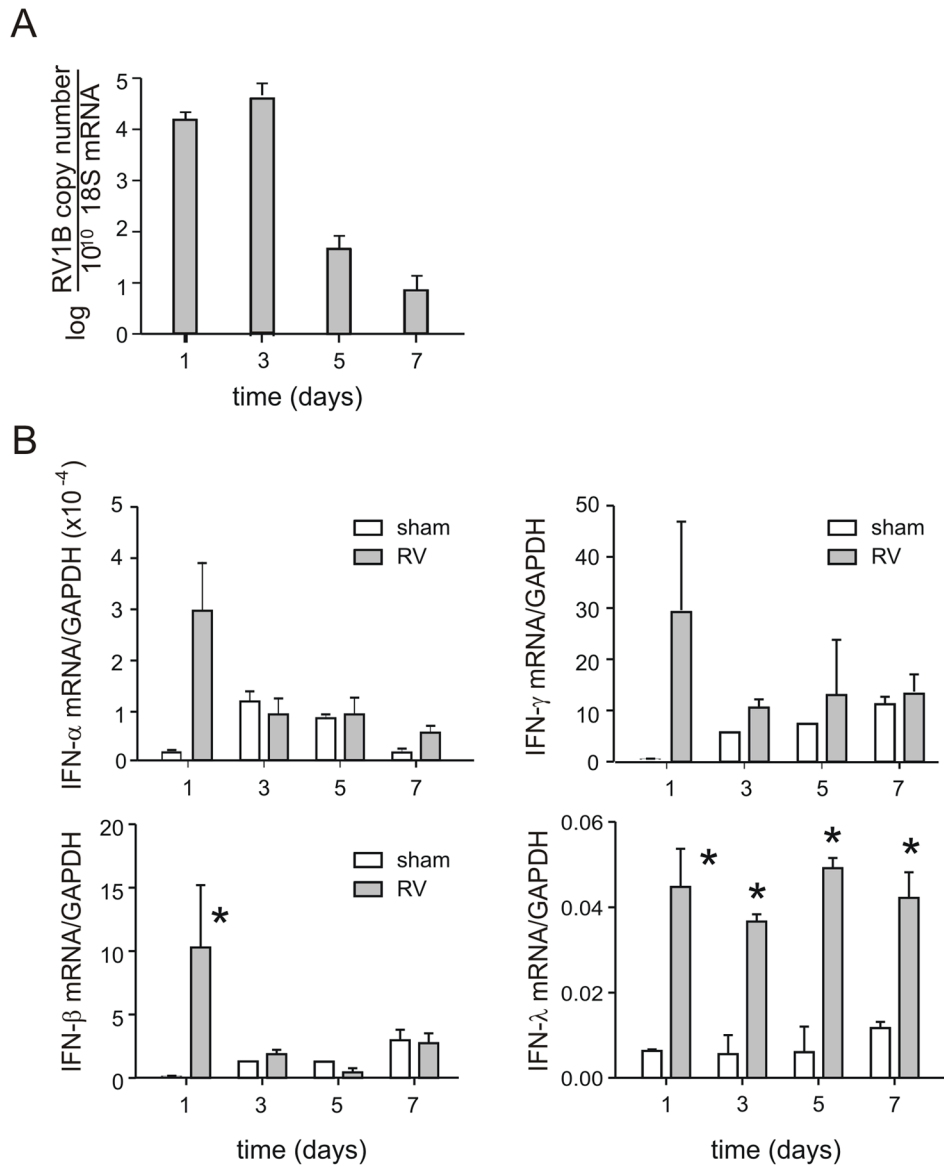
Figure 1. RV1B infection of neonatal mice elicits a brisk IFN response

Seven day-old BALB/c pups were intranasally infected with RV1B or sham control, and lungs harvested for analysis 1–7 days after infection. Positive-strand viral RNA (vRNA, panel A) and mRNAs encoding IFNs-α, -β and γ (B) were measured by qPCR. IFN expression was normalized by expression of the housekeeping gene GAPDH. N = 3–5 animals per time point, *different from sham, p<0.05, unpaired t test.
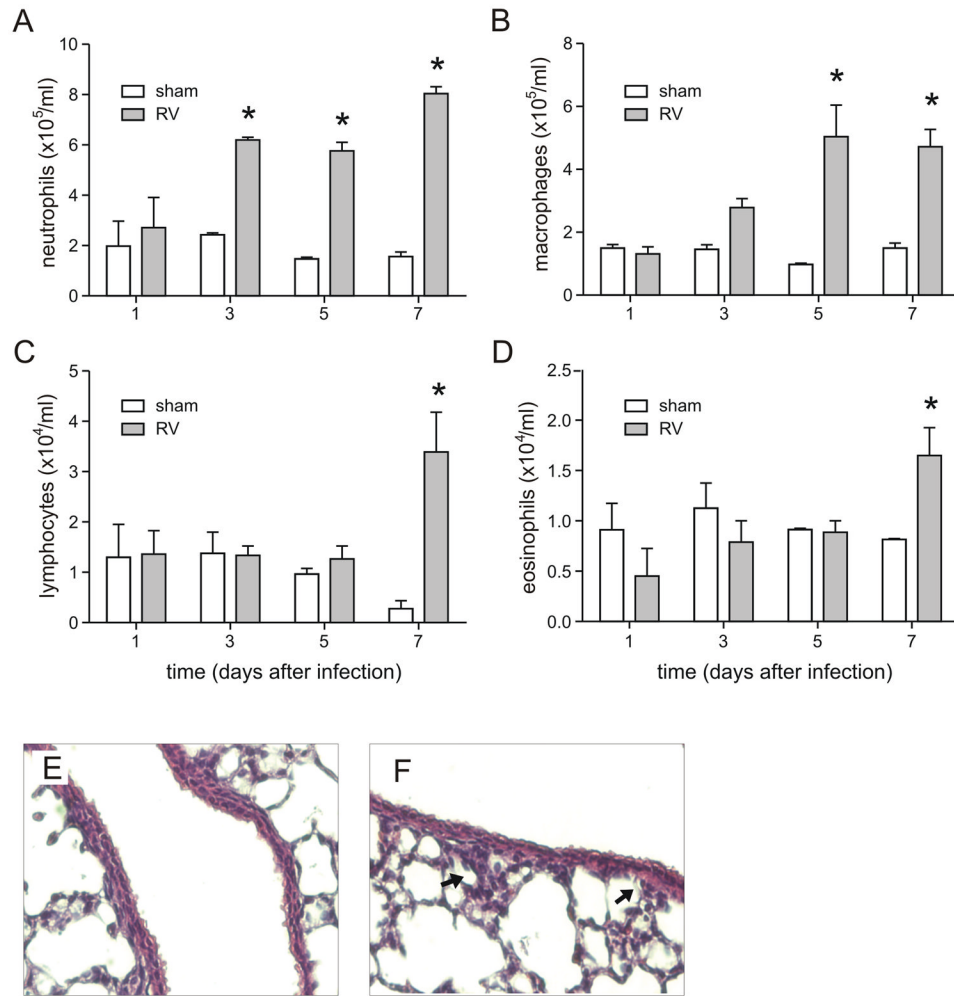
Figure 2. RV1B infection of neonatal mice induces airway inflammation
Seven day-old BALB/c pups were intranasally infected with RV1B or sham control, and lungs homogenates analyzed for inflammatory cell counts (A–D). Cytospins were stained with Diff-Quick. $N = 3–4$ animals per time point, *different from sham, $p<0.05$, unpaired t test. E, F. Images of lungs from sham- (E) and RV1B-infected (F) mice. Lungs were stained with hematoxylin and eosin. Arrows indicate focal areas of inflammation. These images are representative of three individual experiments of three mice per group.
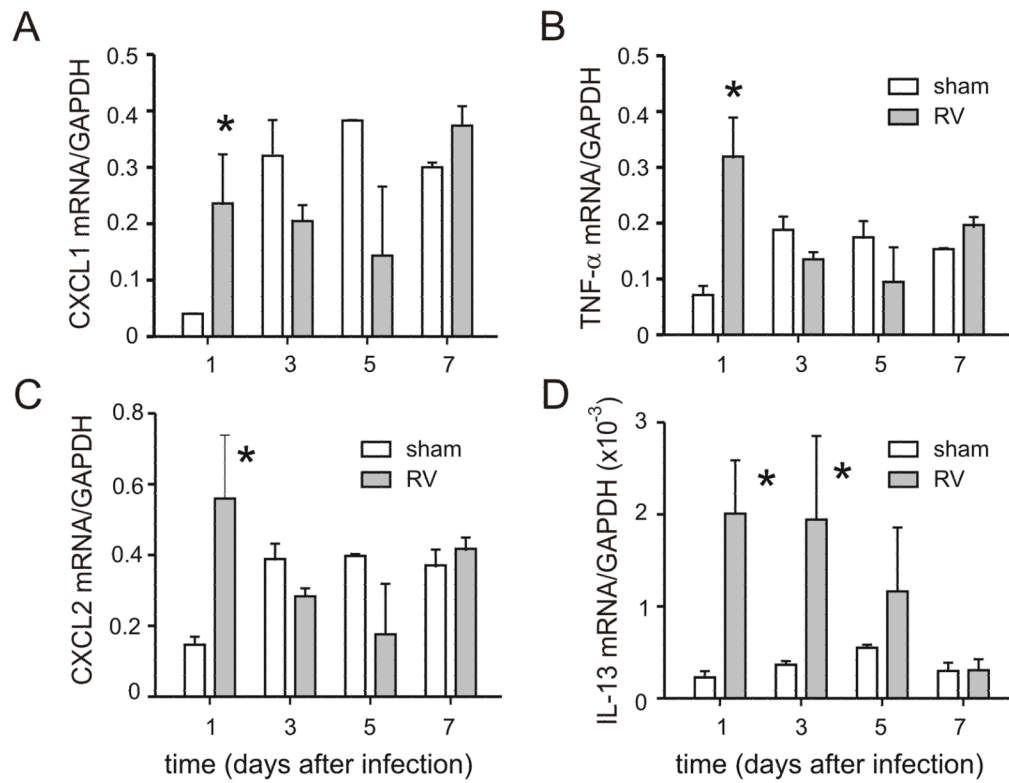
Figure 3.
RV1B infection of 7-day old BALB/c pups increases lung cytokine mRNA levels of CXCL1 (A), CXCL2 (B), TNF-α (C) and IL-13 (D). mRNA expression was measured by qPCR. *N* = 3–10 animals per time point, *different from sham, p<0.05, unpaired t test.
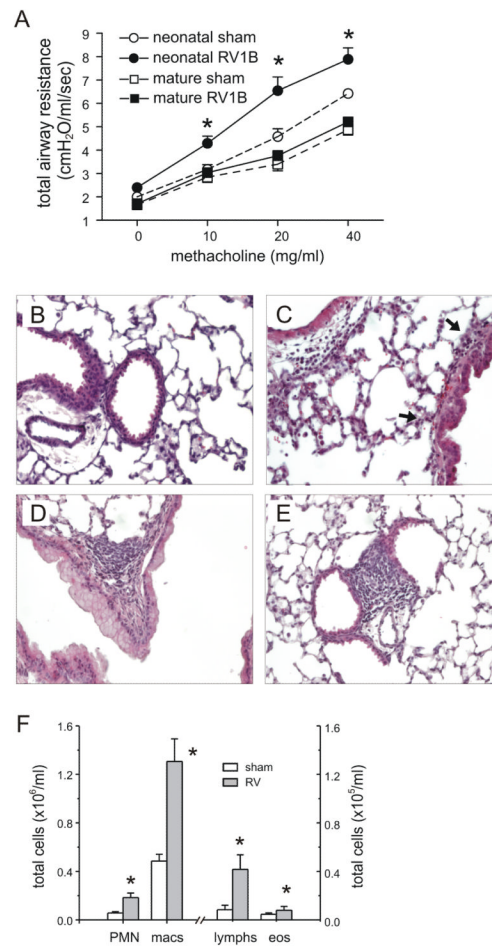
Figure 4.

Neonatal RV infection induces persistent changes in airways responsiveness and inflammation. A. Effects of sham and RV1B infection of neonatal and mature mice on airway cholinergic responsiveness, measured 4 weeks after initial inoculation (day 35 of life for mice infected with RV as neonates and day 84 of life for mice infected with RV at maturity). Airway cholinergic responsiveness was assessed by measuring changes in total respiratory system resistance in response to increasing doses of nebulized methacholine. $N = 6-10$ animals per group, *different from sham-exposed mice of the same age, $p<0.05$, two-way ANOVA. B–E. Representative images of lungs harvested 4 weeks after neonatal sham- (B) or RV1B infection (C–E). Lungs were stained with hematoxylin and eosin. These images are representative of three individual experiments of three mice per group. F. Lung homogenate inflammatory cells from mice harvested 28 days after neonatal inoculation with sham- or RV. Cytospins were stained with Diff-Quick. $N= 6$ animals per group, *different from sham-exposed neonatal mice, $p<0.05$, unpaired t test.

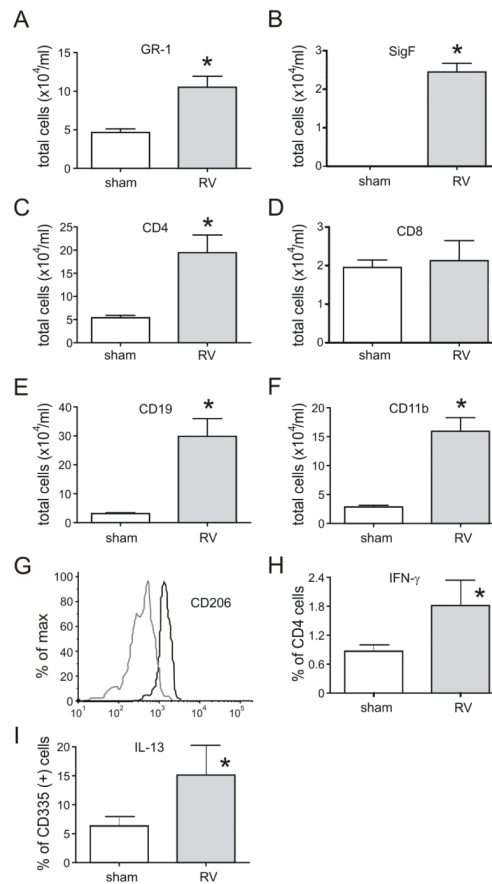**Figure 5.**
Neonatal RV infection induces prolonged changes in airway inflammation. Cells from the minced lungs of 35 day-old mice infected with sham or RV at 7 days of age were analyzed by flow cytometry. Compared to sham-exposed mice, RV-infected mice showed significant increases in (A) Gr1-positive neutrophils and (B) Gr1-, SigF-double-positive and eosinophils, (C) CD4-positive T cells, (E) CD19-positive B cells and (F) CD11b-positive cells. There was no change in the number of CD8-positive cells (D). RV infection increased the CD206 expression of CD11b-positive cells (G; sham, grey line; RV, black line). Lung digests from RV-infected mice showed increases in the percentage of CD4-positive T cells expressing IFN-γ (H) and CD335-positive NK cells expressing IL-13 (I). N = 5–6 animals per group, *different from sham-exposed neonatal mice, $p < 0.05$, rank sum test.
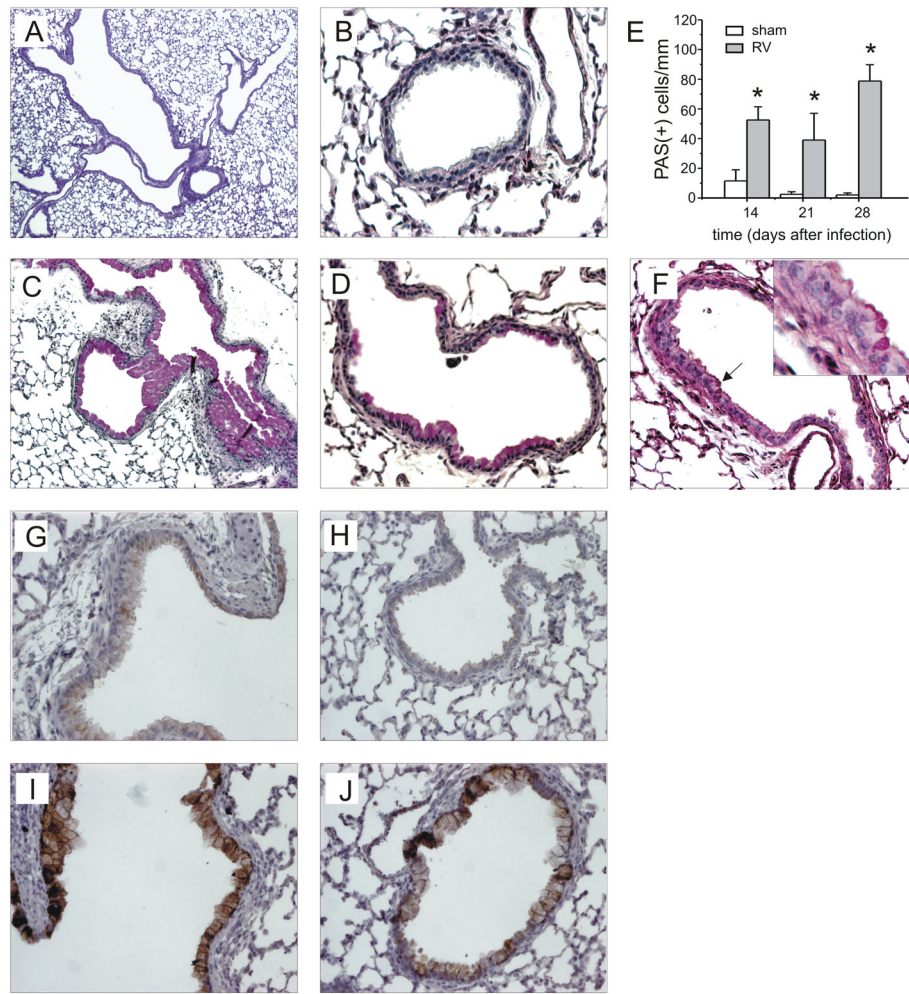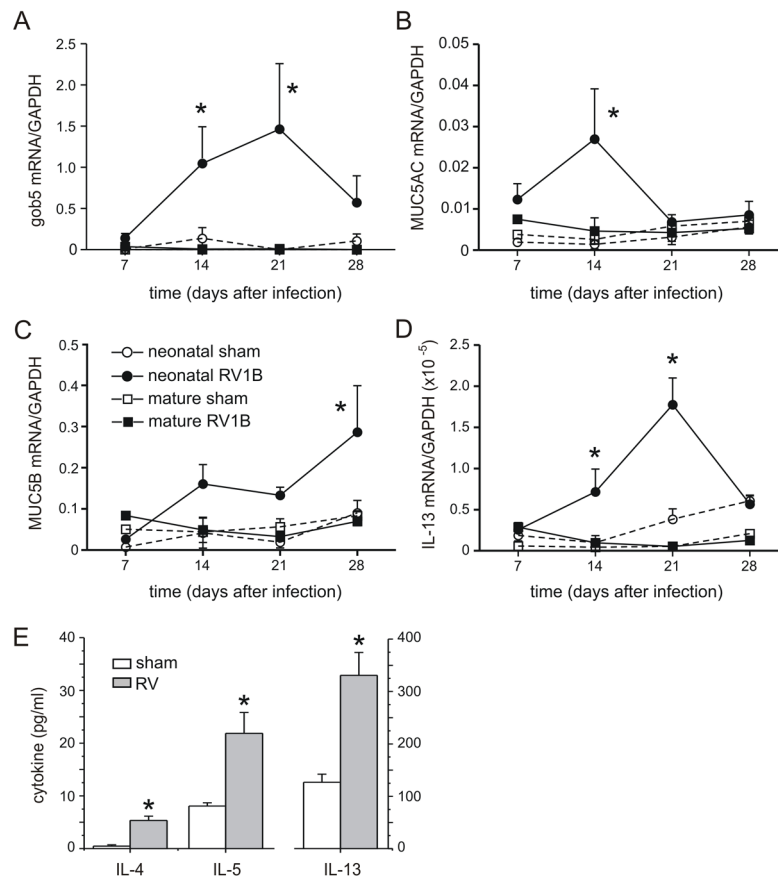
Figure 6.
Neonatal RV infection causes airway mucous metaplasia. Lungs from mice inoculated with sham or RV1B at 7 days age were harvested on day 35 and stained with Periodic acid-Schiff (PAS). PAS staining in the large airways of sham-infected mice ranged from no signal to patches of dense staining (A). Sham-infected animals showed no staining in the small airways (B). In contrast, mice infected at day 7 of life showed some large airways which were completely filled with PAS-positive epithelial cells (C), as well as PAS-staining in the medium-sized and small airways (D). These images are representative of four individual experiments of 4–5 mice per group. E. PAS staining was quantified by using NIH ImageJ analysis software. RV-infected mice showed significantly increased PAS staining 14, 21 and 28 days after infection. $N = 3$ animals per group, *different from sham-exposed mice, $p<0.05$, unpaired t test. F. We also examined PAS staining 60 and 100 days after neonatal sham or RV treatment, on days 67 and 107 of life. RV-infected 67 day-old mice continued to show mucus (arrow, inset). These images are representative of two individual experiments of 4–5 mice per group. G–J. Lung tissues from sham-inoculated (G, H) and RV-infected mice (I, J) were also immunostained for MUC5AC. Signals were amplified and visualized using biotinylated anti-IgG and diaminobenzidine as a substrate. These images are representative of four individual experiments of 4–5 mice per group.

Figure 7.
RV1B infection of 7-day old BALB/c pups induces persistent increases in the expression of mucus-related genes (A–C) and IL-13 (D). mRNA expression was measured by qPCR and normalized for GAPDH. $N = 4$ animals per time point, *different from sham-exposed mice of the same age, $p<0.05$, unpaired t test. E. IL-4, IL-5 and IL-13 protein levels from the lungs of RV-infected mice harvested three weeks after neonatal infection were significantly elevated compared to sham-exposed mice. Protein levels were measured by immune bioplex assay. (N = 4–5 animals per group, *different from sham-exposed mice, $p<0.05$, unpaired t test).
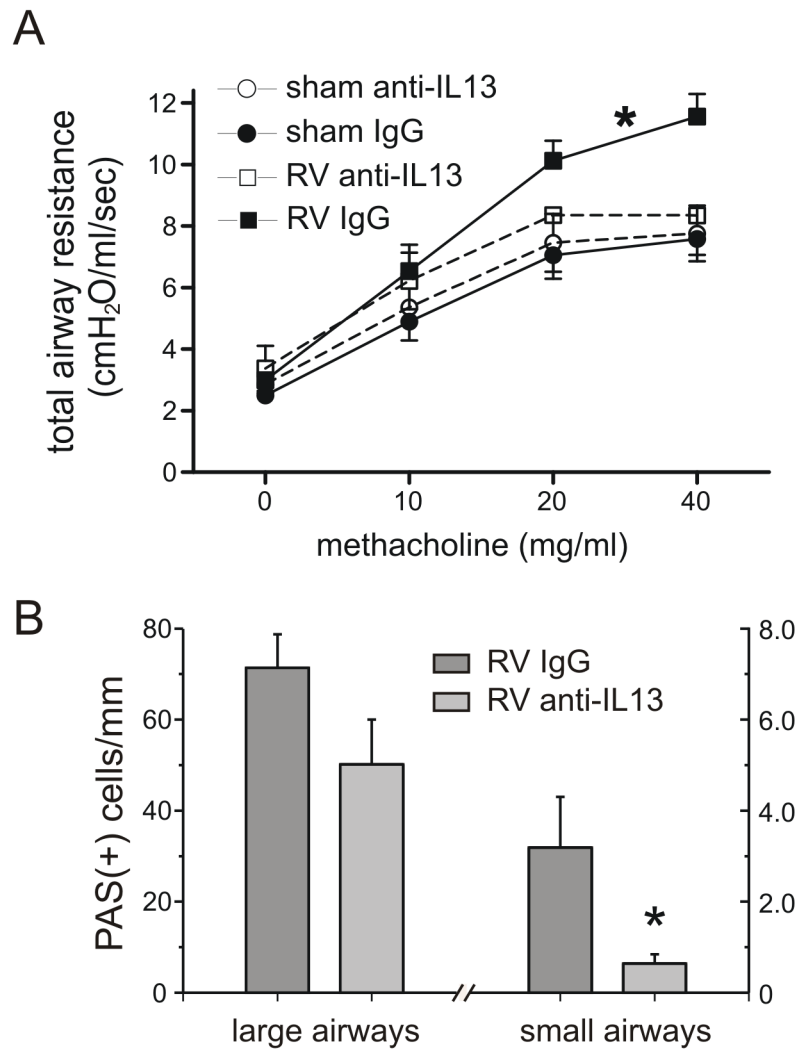
Figure 8.
IL-13 neutralization partially attenuates RV-induced airways hyperresponsiveness and mucous cell metaplasia. A. Sham and RV1B-infected animals were treated with IgG or anti-IL-13. Airway cholinergic responsiveness was measured 4 weeks after initial inoculation. *N* = 4–6 animals per group, *different from sham-exposed mice, $p<0.05$, two-way ANOVA. B. PAS staining in the large and small airways of RV-infected mice treated with anti-IL13 or IgG. *N* = 6–8 animals per group, *different from sham-exposed mice, $p<0.05$, unpaired t test.
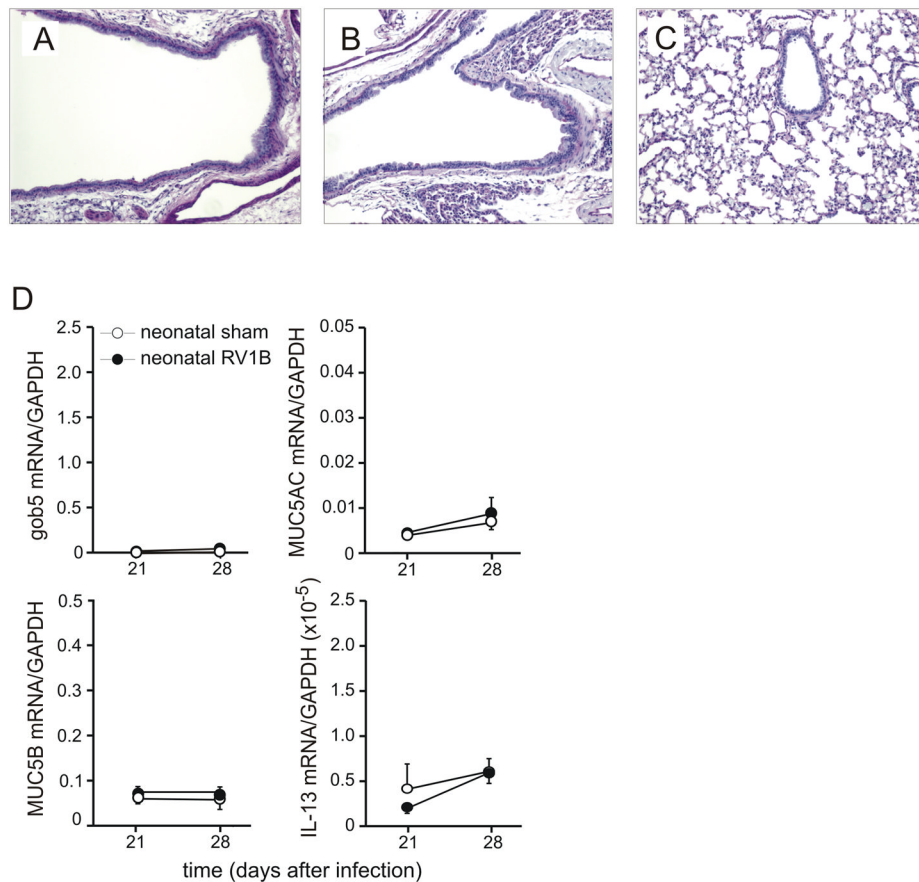
Figure 9.
Effect of neonatal RV infection on IL-4R null mice. BALB/c-*Il4ra^{tm1Sz}*/J mice were inoculated with sham or RV at day 7 of life and airway tissues examined 28 days post-infection. Unlike RV-infected wild-type BALB/c mice (see Figure 6), IL-4R null mice showed no PAS-positive cells in large, medium or small airways (A–C). These images are representative of two individual experiments of three mice per group. D. Lung Gob5, MUC5AC, MUC5B and IL-13 mRNA expression was measured by qPCR. Unlike wild-type mice (see Figure 7), RV-infected IL-4R null mice failed to show an increase in mucus or IL-13 expression. $N = 3–5$ animals per group.
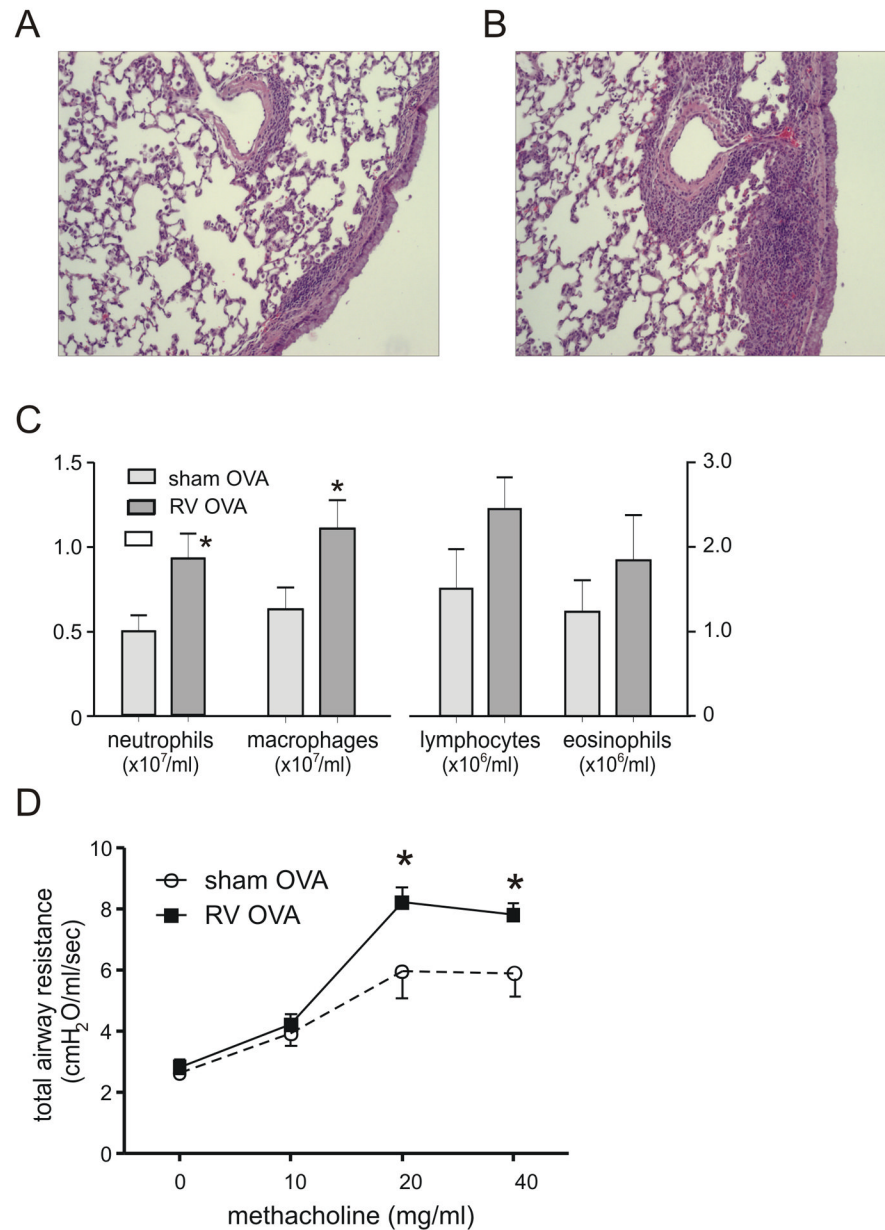
Figure 10.
Effect of neonatal RV infection on the response to allergen sensitization and challenge. Mice were inoculated with sham or RV on day 7 of life, sensitized with intraperitoneal OVA on days 17 and 24 and challenged with intranasal OVA on days 32, 33 and 34. Compared to sham- and OVA-treated mice (panel A), RV-infected, OVA-treated mice showed greater peribronchial inflammation (B). Lung sections were stained with hematoxylin and eosin. Images represent two individual experiments of two mice per group. C, D. RV-infected mice also show greater OVA-induced bronchoalveolar neutrophils and macrophages (C) and airways cholinergic responsiveness (D). $N = 3$–6 animals per group, *different from sham, $p<0.05$, unpaired t test.